Wind and Structures, *Vol. 19, No. 3 (2014) 321-337*
DOI: http://dx.doi.org/10.12989/was.2014.19.3.321

Enhanced remote-sensing scale for wind damage assessment

Jianjun Luo[*1,2], Daan Liang[1a], Cagdas Kafali[2b], Ruilong Li[2c] and Tanya M. Brown[3d]

[1]National Wind Institute, Texas Tech University, 2500 Broadway, Lubbock, TX 79409, USA
[2]AIR Worldwide, 131 Dartmouth Street, Boston, MA 02116, USA
[3]Insurance Institute for Business and Home Safety, 5335 Richburg Road, Richburg, SC 29729, USA

(Received March 28, 2014, Revised June 24, 2014, Accepted July 24, 2014)

Abstract. This study has developed an Enhanced Remote-Sensing (ERS) scale to improve the accuracy and efficiency of using remote-sensing images of residential building to predict their damage conditions. The new scale, by incorporating multiple damage states observable on remote-sensing imagery, substantially reduces measurement errors and increases the amount of information retained. A ground damage survey was conducted six days after the Joplin EF 5 tornado in 2011. A total of 1,400 one- and two-family residences (FR12) were selected and their damage states were evaluated based on Degree of Damage (DOD) in the Enhanced Fujita (EF) scale. A subsequent remote-sensing survey was performed to rate damages with the ERS scale using high-resolution aerial imagery. Results from Ordinary Least Square regression indicate that ERS-derived damage states could reliably predict the ground level damage with 94% of variance in DOD explained by ERS. The superior performance is mainly because ERS extracts more information. The regression model developed can be used for future rapid assessment of tornado damages. In addition, this study provides strong empirical evidence for the effectiveness of the ERS scale and remote-sensing technology for assessment of damages from tornadoes and other wind events.

Keywords: tornadoes; damage assessment; remote-sensing; enhanced remote-sensing scale; Enhanced Fujita scale; degree of damage

1. Introduction

Tornadoes can cause severe damage to buildings, and it is critical to assess damage and losses as quickly as possible to assist post-disaster response and reconstruction (Bunting and Smith 1993, Changnon 2001, Simmons and Sutter 2011). However, in most cases, estimating property damage is challenging, in part because of complex field situations and the lack of standard methods for data collection (Gall *et al*. 2009). Ground surveys have traditionally been regarded as the means for providing reliable information because when investigators have access to the actual situation they are often able to view damage to structures from different angles. However, ground surveys are time-consuming and costly. In addition, after a major disaster, many roads may be badly

∗Corresponding author, Ph.D., E-mail: jluo@air-worldwide.com
[a] Associate Professor, E-mail: daan.liang@ttu.edu
[b] Ph.D., E-mail: ckafali@air-worldwide.com
[c] Ph.D., E-mail: rli@air-worldwide.com
[d] Ph.D., E-mail: tbrown@ibhs.org

http://www.techno-press.org/?journal=was&subpage=8 ISSN: 1226-6116 (Print), 1598-6225 (Online)

damaged or blocked, preventing investigators from approaching objects of interest for close examination. In recent years, satellite and aerial imagery has been used to assess damage after natural disasters including tornadoes. Nevertheless, limitations exist because remote sensed imagery usually only provide information on building roofs, and often lack data on other key components, such as windows, doors, and connections. With continuous improvements in image resolutions and processing algorithms (e.g., the spatial resolution from Landset-1 launched in 1972 is 80 m, that from IKONOS launched in 1999 is 1 m, that from QuickBird launched in 2001 is 0.61m, and that from WorldView-2 launched in 2009 is further improved to 0.46 m), remote-sensing-based tools have a great potential for becoming the next generation solutions to rapid post-tornado damage assessment.

This study proposes a new Enhanced Remote-Sensing scale (ERS scale) to better measure roof damage with remote-sensing imagery. Whether the new scale could improve the accuracy in predicting the overall degree of damage (DOD) of buildings is investigated with statistical model focused on future rapid and cost-effective assessment of windstorm damage to residential buildings. This study provides strong empirical evidence for the usefulness and effectiveness of the ERS scale in tornado and other wind hazard (e.g., straight-lines wind and hurricanes) applications.

The remainder of the paper is organized as follows: Section 1 reviews previous literatures on damage estimates, advantages of remote-sensing technology, and past efforts in constructing remote-sensing scales. At the end of Section 1, an Enhanced Remote-Sensing scale is proposed. Section 2 introduces the methodology used in this study, with discussions in dataset, the Enhanced Remote-Sensing scale, and statistical methods. The results are presented in Section 3 and discussed in Section 4. Finally, conclusions and comments on future work are presented in Section 5.

1.1 Ground-based damage survey

After significant disasters, ground-based survey teams are often deployed to collect detailed and perishable damage data. However, they are time-consuming, labor intensive, and resource demanding (Brown *et al.* 2012, Brown 2010, Speheger *et al.* 2002). It is also difficult to attain a comprehensive view of a large event without the help of remote-sensing images (Molthan *et al.* 2011). Additionally, there are concerns about the quality and feasibility of ground-based efforts. For example, when verifying the documents from the survey of tornadoes of 3 May 1999 in central Oklahoma, Speheger *et al.* (2002) have found the data from ground surveys were not always the best record of the events; eyewitness descriptions, video evidence, and high-resolution remote-sensing data could provide more substantial evidence for tornado evolution and damage.

With new technologies such as personal data assistants (PDA), GPS video camera survey system (Womble *et al.* 2006), damage assessment toolkit (DAT) (Camp *et al.* 2014), as well as appropriate sampling methods (Liang *et al.* 2012), ground surveys can be completed more efficiently. Nevertheless, response time and coverage could still pose challenges. Only after roads are cleared of debris and power lines could investigators be dispatched to the field for data collection and perishable damage data may have been lost to cleanups. Furthermore, there are always some areas which cannot be accessed on the ground due to natural or legal obstacles. Moreover, the subsequent data processing and analysis can consume substantial amounts of time and resources. Thus, alternative methods are needed to supplement or replace the ground-based approach.

1.2 Remote-sensing based damage assessment

In recent years, remote-sensing techniques have advanced and start to play an increasingly important role in assessing damage after natural disasters (Dong and Shan 2013, Joyce *et al.* 2009, Voigt *et al.* 2007). Information with different levels of details can be collected rapidly, typically within 72 hours after the events, at a relatively low cost (Battersby *et al.* 2012). In the context of disaster assessment, remote-sensing usually refers to two specialized techniques, i.e., aerial and satellite remote-sensing, named after the platform from which data are acquired (Khorram *et al.* 2012).

There are many applications of remote-sensing and image processing techniques for prediction and assessment of natural hazards including earthquakes, hurricanes, wildfires, tornadoes etc., and a considerable amount of research has been taken (Davidson 2013, Geiß and Taubenböck 2013, Joyce *et al.* 2009). For example, Eguchi *et al.* (2001) have developed a change detection algorithm based on difference, correlation, and coherence from optical SPOT and SAR ERS satellite imagery before and after the 1999 Marmara earthquake. With certain critical characteristics (hue, saturation, brightness and edge intensity) of building damage, Hasegawa *et al.* (2000) have proposed an automated detection method of damaged buildings from aerial HDTV images taken after the 1995 Kobe earthquake. Bertinelli and Strobl (2013) have studied the impacts of hurricanes on local economic activities by analyzing the relationship between hurricane destruction and local economic activities measured by satellite imagery of nightlights.

There are two types of remote-sensing data commonly used in tornado damage assessment: pre-event and post-event datasets. Pre-event data refers to images taken before a tornado touchdown and can serve as the reference when "before" and "after" images are compared to detect changes. Those images indicate the geographic distribution of buildings, vehicles, trees and other objects, as well as dimension, orientation, and other factors of those objects (Davidson 2013). Post-event data refers to images collected after a tornado.

Even though both of them are desirable, post-event data alone is more widely used when the pre-event data are unavailable, they fail to match, fast initial damage assessment and rapid responses are required, and/or human visual interpretation is adopted (Dong and Shan 2013). For example, with visual interpretation, Brown *et al.* (2012) have performed remote-sensing surveys on the 2008 "Super Tuesday" tornado from two sets of satellite images (one was taken 3 days after the event and the other 5 days after) and 2005 Hurricane Katrina from two sets of aerial images following the event. By tracking debris deposit, Radhika *et al.* (2012) have identified tornado damage paths using a texture-wavelet analysis method from post-storm aerial images of the 2006 Saroma, Japan EF3 tornado.

Nevertheless, the development of remote-sensing technology for rapidly assessing damage after windstorms is still in its infancy, slowed significantly by a fundamental limitation for satellite and aerial images: they primarily display the condition of roofs and not of walls, windows, and doors. Thus, it is important to examine how accurately damage ratings of roofs derived from such imagery could be related to the global condition of buildings.

1.3 Remote-sensing damage scale

Researchers have examined the relationship between damage ratings of roofs assessed based on remote-sensing imagery and damage ratings of overall buildings based on ground-based field surveys (Brown *et al.* 2012). Such a relationship is evident because roof damage has a strong correlation with the overall building damage when the structure is subject to extreme wind loading (Minor 2005, Pinelli *et al.* 2004, Simiu and Scanlan 1996, Womble 2005). To aid such efforts, Womble (2005) developed a Remote-Sensing (RS) damage scale for residential structures. The four-level scale assigns a damage rating, i.e., A, B, C, and D, to the roof based on the most severe damage observed. Table 1 shows the description of each RS damage rating.

Although Womble (2005) did not examine the relationship between the damage states of roofs observed by remote-sensing and those of overall buildings by ground surveys, inherent linkages between those two damage states is intuitive. Based on the definition given by the HAZUS-MH Hurricane (FEMA 2013, Vickery *et al.* 2006), the four states defined in the RS scale are comparable to the description of roof element of the damage states in HAZUS where RS-A corresponds to HAZUS-0 (No damage or very minor damage), RS-B corresponds to HAZUS-1 (Minor damage), RS-C corresponds to the combined HAZUS-2 (Moderate damage) and HAZUS-3 (Severe damage), and RS-D corresponds to HAZUS-4 (Destruction).

To characterize the relationship between the damage states of roofs observed by remote-sensing and those of overall buildings by ground surveys, Brown *et al.* (2012) have used a dataset of damage states (both ground-based damage data and matched remote-sensing damage data from high resolution satellite imagery) of 271 one- and two-family residences (FR12) from the “Super Tuesday” tornado in 2008. Realizing that Womble’s four-level damage rating scale was often too coarse to describe damage states of the roof, they propose an alphanumeric scale by adding a parameter into the initial RS scale to specify the percentage of damaged area. Damage assessed based on this modified RS scale could explain 68.6% of variance in ground survey based damage in the best model presented in the study (R^2=68.6%) (Brown *et al.* 2012).

Notably, RS scales in Womble (2005) and Brown *et al.* (2012) are based on the most severe damage observed, and thus could not utilize potentially valuable information about the different states of damage at different parts of a roof. When the damage of a small part of the building, i.e., the roof, is used to predict the overall damage of the whole building, the adequacy of information is always in question. Additionally, previous damage descriptions of RS scale would not be well suited for automated image processing and damage detection.

Table 1 Description of Womble’s Remote-Sensing (RS) damage scale for residential structures (Womble 2005)

Damage Rating	Description of most severe physical damage
RS-A	No apparent damage
RS-B	Shingles/tiles removed, leaving decking exposed
RS-C	Decking removed, leaving roof structure exposed
RS-D	Roof structure collapsed or removed. Walls may have collapsed

1.4 Enhanced remote-sensing scale and environmental factors

This study proposes a new Enhanced Remote-Sensing scale (ERS) to rate building damages using remote-sensing images for improved prediction of ground damages. Consistent with the scales developed by Womble (2005) and Brown *et al*. (2012), the ERS scale uses A, B, C, D classification and the percentage of damage observed. In addition, the ERS scale not only considers the most severe damage but also tries to include all the damage states observed. For example, the classification of D with 1-25% of damage is further augmented with information on how much B and C damage was observed. In doing so, the ERS scale has been expanded to 36 levels of damage, as explained in the Subsection 2.2.2, whereas the previous RS scales have up to four levels of damage (Womble 2005) or 13 levels of damage (Brown *et al*. 2012).

The ERS scale improves on previous scales by using not only the maximum damage state of roofs but incorporating all damage states extracted from remote-sensing imagery and thus substantially reduces errors in assessing damage states. Accordingly, it is expected that the new scale is able to more accurately predict ground damage than previous ones.

Additionally, the information on surrounding damage and debris is included to strengthen ground level damage prediction. As certain aspects of wind damage are not commonly captured by overhead imagery, such as damages to doors, windows, and walls, debris field and surrounding damage defined as surrogate damage indicators by Womble (2005) could function as extra indicators for providing further information about the damage status of buildings of interest and reducing uncertainty in the damage prediction.

2. Methodology

2.1 Data collection and processing

An EF 5 tornado occurred in Joplin, Missouri on May 22, 2011, which resulted in devastating building damages, 158 fatalities and over 1,000 injuries. The Joplin tornado was considered the costliest and the 7th deadliest tornado in U.S. history to date. The maximum estimated wind speed exceeded 322 km (200 mph). The track length and width were estimated at 35.6 km (22.1 miles) and 1.2 km to 1.6 km (3/4 to 1 miles) respectively (NWS 2011).

Six days after the Joplin tornado, a damage assessment team from the National Wind Institute (NWI) of Texas Tech University (TTU) was deployed. It spent four days travelling over 138 km within affected areas and recording 14 hours of high-definition ground level video for over 6,000 buildings with two GPS-enabled video cameras. Later, 50,435 images were extracted and archived in an ArcGIS database. Fig. 1 shows the geographic distribution of 6,579 buildings observed in the survey, overlaid with storm intensities determined by the National Weather Service. Data acquired from other sources such as building and parcel information, fatalities, historical records of tornadoes in the study areas, census, as well as satellite and aerial images were also added to the ArcGIS database.

Using the database, damage states of 6,579 buildings observed in the ground survey images were manually assessed according to the Degree of Damage (DOD) in the EF scale (WISE 2006). 1,400 one-and two-family residences (FR12) were selected to be further rated using remote-sensing imagery. The ERS was assigned by visual interpretation, utilizing 0.1 m spatial resolution post-event aerial imagery taken approximately 10 days after the tornado (Source: the Geographic Information Services of Jasper County, Missouri). Pre-event aerial imagery with spatial resolution of 0.15 m taken in 2009 was also made available as the benchmark.

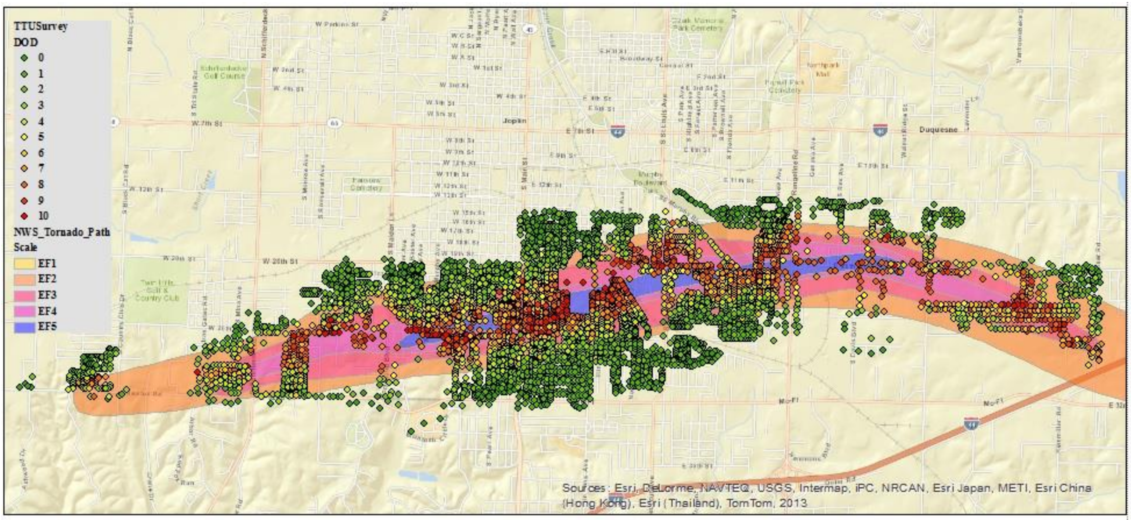

Fig. 1 Buildings included in the ground survey across the tornado path as determined by the National Weather Service (NWS) Source of the track shown in Fig. 1:NWS (2011)

2.2 Measures of building damages

2.2.1 Damage states of the overall building: Degree of Damage

The overall damage state of a building is indicated by the numerical Degree of Damage (DOD). Table 2 shows the definition of each DOD as well as associated wind speeds according to WISE (2006). For example, Fig. 2 shows the ground imagery of two residential structures damaged by 2011 Joplin tornado (the overhead imagery of these buildings are shown in Fig. 3). The building in Fig. 2(a) is rated as DOD 4 because more than 20% of the roof covering material was lost and the garage door collapsed inward. The building in Fig. 2(b) is rated as DOD 6 because large sections of the roof structure were removed, but most walls remained standing.

(a) DOD = 4 (TTU #687) (b) DOD = 6 (TTU #254)

Fig. 2 Ground imagery of two residential structures damaged by 2011 Joplin tornado (Source: Photographs taken with GPS video camera survey system by NWI of TTU)

Table 2 Description of Degree of Damage (DOD) for one-and two-family residences (FR12) (WISE 2006)

DOD	Damage Description	Expected wind speed* (mph)	Lower bound wind speed* (mph)	Upper bound wind speed* (mph)
1	Threshold of visible damage	65	53	80
2	Loss of roof covering material (<20%), gutters and/or awning; loss of vinyl or metal siding	79	63	97
3	Broken glass in windows and doors	96	79	114
4	Uplift of roof deck and loss of significant roof covering material (>20%); collapse of chimney; garage doors collapse inward or outward; failure of porch or carport	97	81	116
5	Entire house shifts of foundation	121	103	141
6	Large sections of roof structure removed; most walls remain standing	122	104	142
7	Exterior walls collapse	132	113	153
8	Most walls collapsed in bottom floor, except small interior rooms	152	127	178
9	All walls collapsed	170	142	198
10	Destruction of engineered and/or well-constructed residence; slab swept clean	200	165	220

* The wind speeds shown in this table are 3-second gust speeds in mph (mile per hour)

2.2.2 Damage states of the roof: the Enhanced Remote-Sensing scale

Damage state of a building’s roof is measured with an Enhanced Remote-Sensing (ERS) scale. The numerical values of the ERS range from 0 to 10, corresponding to 36 discrete damage states as shown in Table 3.

Table 3 The Enhanced Remote-Sensing scale for FR12

State No.	ERS Category	Numerical Value
1	A	0
2	B 1-25%	1
3	B 26-50%	2
4	B 51%-75%	2.286
5	B >75%	2.571
6	C 1-25% B 1-25%	2.857
7	C 1-25% B 26-50%	3.143
8	C 1-25% B 51-75%	3.429
9	C 1-25% B >75%	3.714
10	C 26-50% B 26-50%	4
11	C 26-50% B 51-75%	4.125
12	C 26-50% B >75%	4.25
13	C 51-75% B 51-75%	4.375
14	C 51-75% B >75%	4.5
15	C >75% B >75%	4.625
16	D 1-25% C 1-25% B 1-25%	4.75
17	D 1-25% C 1-25% B 26-50%	4.875
18	D 1-25% C 1-25% B 51%-75%	5
19	D 1-25% C 1-25% B >75%	5.125
20	D 1-25% C 26-50% B 26-50	5.25
21	D 1-25% C 26-50% B 51-75%	5.375
22	D 1-25% C 26-50% B >75%	5.5
23	D 1-25% C 51-75% B 51-75%	5.625
24	D 1-25% C 51-75% B >75%	5.75
25	D 1-25% C >75% B >75%	5.875
26	D 26-50% C 26-50% B 26-50%	6
27	D 26-50% C 26-50% B 51-75%	6.333
28	D 26-50% C 26-50% B >75%	6.667
29	D 26-50% C 51-75% B 51-75%	7
30	D 26-50% C 51-75% B >75%	7.333
31	D 26-50% C >75% B >75%	7.667
32	D 51-75% C 51-75% B 51-75%	8
33	D 51-75% C51-75% B >75%	8.333
34	D 51-75% C >75% B >75%	8.667
35	D >75% C >75% B >75%	9
36	Slab swept clean	10

The ERS scale combines an alphabetic RS scale with an indicator of the percentage of damage area. It uses A, B, C, D to describe damage observed, following Womble (2005), and it also specifies the percentage of damage (1-25%, 26-50%, 51-75%, and >75%) related with each level of damage, following Brown *et al*. (2012).The ERS scale uses a more granular characterization of roof damage, taking into account a building might experience multiple levels of damage. Consequently, there were a total of 36 damage states defined in the scale.

The numerical values of the ERS are determined according to intrinsic relationship with the DOD. First, six key damage states of ERS are identified, namely "A", "B 26-50%", "C 26-50% B 26-50%", "D 26-50% C 26-50% B 26-50%", "D >75% C >75% B >75%", and "Slab swept clean". Those states are assigned numerical values of 0, 2, 4, 6, 9, and 10 to match the same numerical values as defined in the DOD. After that, linear interpolation is applied to calculate proper numerical values for the remaining 30 damage states.

Fig. 3 shows the aerial imagery of the same two residential structures presented in Fig. 2. The roof damage states of these two buildings are rated with ERS, which is summarized in Table 4. In addition to the ERS rating, ratings based on RS scales from Womble and Brown *et al.* are also provided to highlight their differences. For Fig. 3(a), because the most severe damage located at the middle of the roof is "Decking removed, leaving roof structure exposed", Womble would rate the roof as C level damage. Brown *et al.* would further consider the percentage of this most severe damage area in the roof, which is 1-25%, and rate the roof damage as "C 1-25%". Using ERS scale, the building is rated as "C 1-25% B 51-75%" because about 51% to 75% of "the shingles removed and leaving decking exposed". For Fig. 3(b), the building is rated as "D 1-25% C >75% B >75%" based on the ERS since there were less than 25% roof structure removed at the bottom left corner, almost all the roof structure exposed, and all the singles/tiles removed from the roof. In contrast, the building would be rated as D and "D 1-25%" based on Womble and Brown *et al.* respectively.

(a) ERS Rating: "C 1-25% B 51-75%" (TTU #687)

(b) ERS Rating: "D 1-25% C >75% B >75%" (TTU #254)

Fig. 3 Aerial imagery of two residential structures damaged by 2011 Joplin tornado (Source: the Geographic Information Services of Jasper County, Missouri)

Table 4 Results from three different damage rating systems

Sample	RS (Womble)	RS (Brown *et al.*)	ERS
(a) TTU #687	C	C 1-25%	C 1-25% B 51-75%
(b) TTU #254	D	D 1-25%	D 1-25% C >75% B >75%

2.3 Analysis and validation

Ordinary Least Regression is used to estimate the relationship between ground-based damage rating characterized by DOD using EF Scale and remotely-sensed damage rating characterized by the newly developed ERS scale. Goodness-of-fit of the model is evaluated with coefficient of determination (R^2).

When ERS is 0 (i.e., no damage is visually detected from the remote sensed image), the actual condition of the building could fall into one of the following two possible cases:

- The building sustains minor damage, but the roof shows no damage or minor damage that is difficult to detect with visual examination. In this case, even though ERS is 0, the actual DOD of the building should not be 0;
- The building is not damaged by the tornado at all whether it is located outside or inside the tornado track. In this case, both ERS and DOD ought to be 0.

As the purpose of this study is to evaluate the capability of the ERS scale to rapidly and reliably assess tornado damage of buildings using remote-sensing images, buildings located far outside the track are removed from the sample set. However, for buildings located near the boundary of the track, it is reasonable to assume that ones with ERS 0 and no surrounding debris or building damages are likely to sustain no wind damage. Here an indicator is used to record whether debris or damage observed within a 20 meter radius around the subject. As the result, additional 82 buildings meeting such a criterion are removed from the sample set. The regression analysis is conducted on the constrained sample set of 1,318 FR12 buildings.

The model is validated with splitting sample validation. The dataset is randomly divided into two parts, with one part used as the training set to train a model and the remaining part used as the test set to examine the accuracy of the model. Because single data splitting is not reliable, ten-fold cross-validation is often practiced (Harrell 2001). For the ten-fold cross-validation, the dataset is divided into 10 groups, with nine of them used to train a model and the remaining one used to validate the model. Furthermore, to reduce variability, validation is usually repeated multiple times and the indicators for the accuracy (e.g., R^2 in OLS regression) are averaged (Cassell 2007, Harrell 2001).

In this study, ten-fold cross-validation is used and repeated 1,000 times for better precision. The R^2 was averaged across all the 1,000 test sets. A minimum decrease of R^2 from the best-fit-model would indicate robustness of the model.

3. Results

Figs. 4(a)-4(c) presents the univariate and bivariate distribution of ERS numerical value (abbreviated subsequently as ERS) and DOD. ERS was concentrated on the lower levels of damage (0-2) while DOD was concentrated on the lower levels of damage (1-4). Correspondingly, the bivariate distribution was skewed toward the lowest levels of DOD and ERS.

Table 5 presents regression results. The model could be written as

$$\mathrm{DOD} = 1.075 + 0.853\mathrm{ERS} + \varepsilon \tag{1}$$

where ε is a random error.

The model had a high R^2, which means the model could explain 94.3% of variance in DOD, suggesting ERS is a strong predictor for DOD with high accuracy.

Fig. 5 presents the 95% confidence limits and the prediction limits of the DOD based on ERS along with the actual observation. It helps to visualize the accuracy of using ERS to predict DOD. The confidence limits show the interval estimate of the mean; these limits are very small, and thus are not visible in the plot. The prediction limits show the interval estimate of data observations. In the model, most observations of DOD fall within the prediction limits; furthermore, there is a strong linear trend between ERS and DOD.

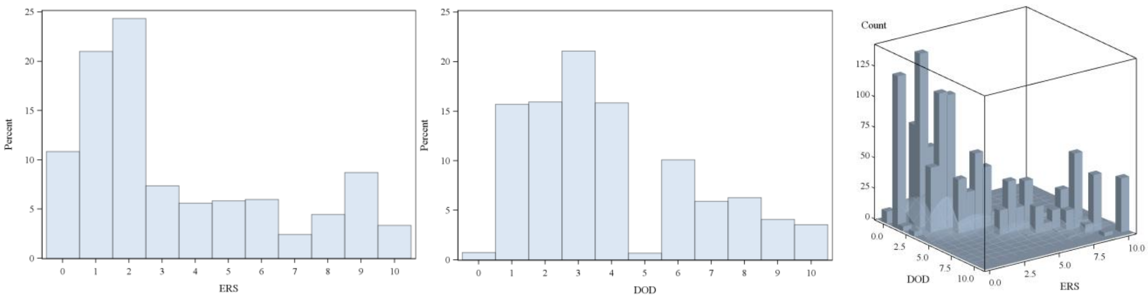

(a) Univariate distribution of ERS (b) Univariate distribution of DOD (c) Bivariate distribution of ERS and DOD

Fig. 4 Univariate and bivariate distribution of ERS and DOD

Table 5 Regression of DOD on ERS damage state

	Coefficient	Standard Error	p Value
ERS	0.853	0.006	<0.0001
Constant	1.075	0.026	<0.0001
N	1318		
F (DF)	21693.1 (1)		<0.001
R^2	0.943		

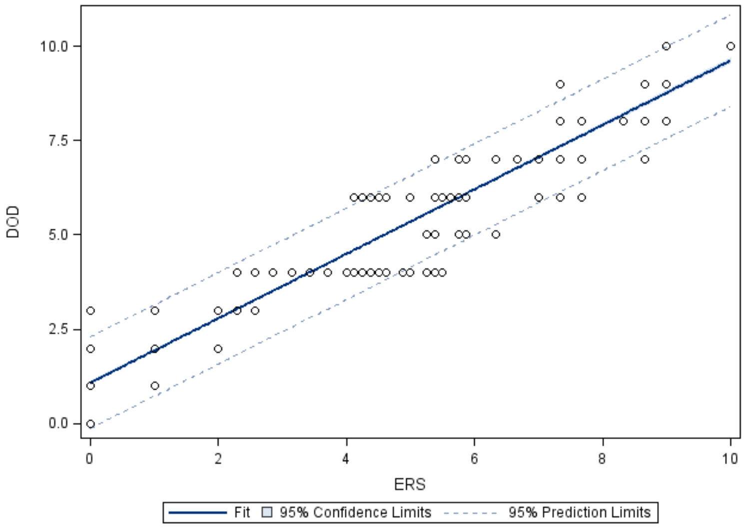

Fig. 5 Statistical relationships between ERS damage state and DOD in windstorm with 95% confidence interval and prediction interval

The model is validated with the ten-fold cross-validation repeated 1,000 times. The validation results in an average R^2 of 0.942 across all the 1,000 test sets, which is almost identical to R^2 of the model. Furthermore, of all those R^2 values generated, the minimum is 0.904, the maximum is 0.970, and the standard deviation is 0.010. Thus, the validation result demonstrates a strong evidence of the model's robustness.

4. Discussion

In this study, an enhanced remote-sensing damage scale (ERS) is proposed to rate residential building damages solely based on remote-sensing imagery. A statistical model is developed to examine the relationships between the roof damage rated by the ERS and the ground truth provided by the EF scale.

The model performs very well. The ERS explained about 94% of the variance in DOD based on ground survey of the damage states of buildings. Especially when the objective is not to assess each individual building's damage but to quantify area wide impact, ERS would be an excellent tool for emergency managers during disaster relief efforts.

The ERS is believed to outperform previous remote-sensing scales for several reasons. First, the ERS is designed to preserve and use additional information extracted from remote sensed imagery by reporting on the damage states of multiple components of a single building. In contrast, RS scales (Brown *et al*. 2012, Womble 2005) only consider the most severe damage observed and lead to the loss of valuable information on lesser damages. As remote-sensing imagery has already been constrained in term of its ability to detect building conditions from the above, extra information provides by the ERS proves intrinsically advantageous.

In addition, the imagery spatial resolution used in this study is higher than that in previous studies using RS scales (Brown *et al.* 2012, Womble 2005). Generally speaking, finer spatial resolution offers more details and greater capability to detect damages. Jensen and Cowen (1999) studied the temporal and spatial resolution requirements for remote-sensing of urban/suburban infrastructure. They recommended a minimum resolution for building and property infrastructure of 0.25 m - 0.5 m. Bolus and Bruzewicz (2002) examined the optimal resolution for differentiating roof structures. They suggested that the resolution of 0.2 m (8 inch) was needed for the differentiation of individual roof rafters. However, Womble (2005) and Brown (2012) only have access to satellite remote-sensing images with limited resolution available at the time when they conducted their studies. Brown *et al.* (2012) uses the remote-sensing imagery with spatial resolutions of 0.5 m and 0.61 m in their study on the 2008 Super Tuesday tornado, less than the suggested resolution. In contrast, the aerial remote-sensing imagery used in this study has a resolution of 0.1 m, well suited for the detailed classification in the ERS.

Furthermore, the dataset used in Brown *et al.* (2012) doesn’t contain sufficient numbers of buildings with high levels of damage and most of the data used for the model fitting were at low and moderate damage states (i.e., DOD 4 or lower, and RS-B or lower) with very few buildings (2%) rated DOD 7 or above, which limited the power of the models. In contrast, this study includes 262 (18.7%) buildings rated as DOD 7 or above, increasing the power of the model in predicting higher levels of damage.

This study also highlights the necessity to include surrounding environment as a sampling technique for delineating the boundary of tornado track. By focusing only on buildings located within the track, the uncertainty in model prediction due to differences in sampling methods is reduced. The model intercept suggests that the expected ground level damage was close to 1 (i.e., threshold of visible damage) even when ERS was 0. This is consistent with field observations as the majority of buildings sustained debris damages to walls or openings not shown on remote-sensing imagery. Thus, the inclusion of the surrounding environment helps increase the performance of the model.

Another advantage of ERS is the clear and simple description of roof damage to minimize human biases. In contrast, DOD has a more complex syntax in which different building components and their damage levels are considered. From our own experience, rating with ERS could approximately be accomplished ten times faster than rating with DOD for a trained evaluator. Furthermore, the inconsistency of the subjective assessment of DOD is always of concern, and often experts do not agree with each other on the level of DOD for same buildings (Edwards *et al.* 2013, NIST 2013).

With a detailed classification structure, the development of ERS is continuing to lay the foundation for automated damage detection. The potential benefit of using remote-sensing to collect information declines with time following a disaster because other methods of collecting information become available (Hodgson *et al.* 2010). The timely analysis of remote-sensing data can be enhanced with automated image processing. But these methods have not yet been fully developed and tested, leaving analyses heavily relying on visual and manual interpretation for the immediate impacts of disasters (Battersby *et al.* 2012, Joyce *et al.* 2009). Lack of robust damage detection algorithms and tools substantially limits the application of remote-sensing technology in hazard monitoring, detection, and evaluation (Joyce *et al.* 2009).

As the aerial damage survey used in the study was conducted 10 days after the tornado, some debris had been removed and minor damage had been repaired, possibly affecting the accuracy of damage assessment for buildings - especially those with low levels of damage. This problem could be mitigated with using earlier imagery from other sources such as FEMA. In general, aerial surveys, that are able to obtain high-resolution imagery, often lag considerably the actual events or are unavailable due to technical and financial challenges. In contrast, satellite-based surveys can cost less and have greater area coverage, although spatial resolution is coarser. Nevertheless, as the technology improves, higher resolution satellite imagery is expected to become available. In addition, other emerging technologies such as unmanned aerial vehicles (UAV) have the potential to become a preferred method for rapid damage survey (Adams *et al.* 2010, Adams *et al.* 2013, Adams and Friedland 2011, DeBusk 2010). These advancements in technology will further strengthen the use of remote-sensing imagery for the rapid assessment of damage.

5. Conclusions

This study proposes an Enhanced Remote-Sensing scale and examines the relationships between roof damage rated with the ERS and the overall condition of the buildings rated with the DOD. The model demonstrates a high capability to predict overall damage of buildings because the ERS scale utilizes more information available in high resolution aerial remote-sensing imagery and thus describes the roof damage with more accuracy.

The study has developed methods and tools that can promote the application of remote-sensing in practice. Remote-sensing has been proposed by researchers as a timely and cost-effective way to assess ground level damage. It is known that roof damage has a strong correlation with overall building damage due to wind; thus it is reasonable to use remote-sensing imagery of roofs to estimate overall building damage. However, broader use of remote-sensing technology in post windstorm damage assessment would call for more robust methods and tools. This study provides strong empirical evidence that remote-sensing can be used to reliably assess building damage states, and the consideration of the surrounding environment substantially increases the accuracy.

One topic of interest is to examine the effectiveness of ERS when applied to other occupancy types (e.g., apartments, motels, malls, mobile home) and construction classes (e.g., wood frame, masonry veneer, concrete, metal). As there are 28 damage indicators (DIs) adopted in the EF scale (WISE 2006), additional datasets could be collected and analyzed, resulting in different models for different types of DIs. In addition, advanced technologies such as oblique imagery heavily used in a recent 2013 Moore, OK tornado are able to identify damage to windows, roof undersides, siding, etc, providing extra pieces of information for the future improvement to ERS

Another topic involves the applicability of ERS in hurricanes and straight-line winds. As failure mechanisms differ, the correlation between RS-derived damage rating and ground truth may vary (Haan *et al.* 2010, Marshall 2008, Simiu and Scanlan 1996). Following similar methodology, datasets collected from events such as Hurricane Katrina and Hurricane Ike could be analyzed. The result may then shed light on transferability of models and parameters across hazard types.

Furthermore, the potential use of ERS to estimate insured loss could be explored. In loss models, insured loss is not linearly correlated with the severity of damage. In the Florida public hurricane loss model, when damage on a residential building exceeds 50%, the total loss will be set to 100% (Hamid 2007). In HAZUS-MH Hurricane, replacement thresholds are defined as the levels beyond which building components should be completely replaced. For example, the replacement thresholds were set at 2.5% for roof covering and at 5% for roof sheathing (FEMA 2013). With a better capability in detecting and classifying minor to moderate damages, the ERS could be well suited to quickly assess the economic losses after a major windstorm.

Acknowledgements

The authors would like to thank Terri Branham, Lin Cong, and Kim Corson for their participation in field data collection. They thank Arn Womble, Yuepeng Cui, Tom Quintero, Pataya Scott, and Kelvin Lee for their assistance in damage ratings. They also thank Chris Chappell, the GIS coordinator of Jasper County, for providing imagery and property data for Joplin. This material is partially based upon work in part supported by the National Science Foundation under Grants CMMI-1000251 and 1131392. Any opinions, findings, and conclusions or recommendations expressed in this paper are those of the authors and do not necessarily reflect the views of the National Science Foundation.

References

Adams, S.M. and Friedland, C.J. (2011), "A Survey of Unmanned Aerial Vehicle (UAV) Usage for Imagery Collection in Disaster Research and Management", *Proceedings of the 9th International Workshop on Remote Sensing for Disaster Response*, Stanford, CA, USA, September.

Adams, S.M., Friedland, C.J. and Levitan, M.L. (2010), "Unmanned Aerial Vehicle data acquisition for damage assessment in hurricane events", *Proceedings of the 8th International Workshop on Remote Sensing for Disaster Management*, Tokyo, Japan, September.

Adams, S.M., Levitan, M.L. and Friedland, C.J. (2012), "High resolution imagery collection utilizing Unmanned Aerial Vehicles (UAVs) for post-disaster studies", *Proceedings of the ATC & SEI Conference on Advances in Hurricane Engineering*, Miami, Florida, USA, October.

Battersby, S.E., Hodgson, M.E. and Wang, J. (2012), "Spatial resolution imagery requirements for identifying structure damage in a hurricane disaster: a cognitive approach", *Photogramm. Eng. Rem. S.*, **78**(6), 625-635.

Bertinelli, L. and Strobl, E. (2013), "Quantifying the local economic growth impact of hurricane strikes: an analysis from outer space for the Caribbean", *J. Appl. Meteorol. Clim*., **52**(8), 1688-1697.

Bolus, R. and Bruzewicz, A. (2002), *Evaluation of new sensors for emergency management*, Technical Report ERDC/CRREL TR-02-11, US Army Corps of Engineers, Engineer Research and Development Center, USA.

Brown, T.M. (2010), *Development of a statistical relationship between ground-based and remotely-sensed damage in windstorms*, PhD Dissertation, Texas Tech University, Lubbock, Texas, USA.

Brown, T.M., Liang, D. and Womble, J.A. (2012), "Predicting ground-based damage states from windstorms using remote-sensing imagery", *Wind Struct*., **15**(5), 369-383.

Bunting, W.F. and Smith, B.E. (1993), "A guide for conducting convective windstorm surveys", NOAA Tech. Memo. NWS SR-146. Sci. Services Div., Southern Region, Fort Worth, TX, USA.

Camp, J.P., Rothfusz, L.P., Anderson, A., Speheger, D., Ortega, K.L. and Smith, B.R. (2014), "Assessing the Moore, Oklahoma (2013) Tornado Using the National Weather Service Damage Assessment Toolkit", *Proceedings of the 94th American Meteorological Society Annual Meeting*. Atlanta, Georgia, USA, February.

Cassell, D.L. (2007), "Don't be loopy: re-sampling and simulation the SAS way", *Proceedings of the SAS Global Forum 2007 Conference*, Orlando, Florida, USA, April.

Changnon, S.A. (2001), "Damaging thunderstorm activity in the United States", *B. Am. Meteorol. Soc*., **82** (4), 597-608.

Davidson, R. (2013), "Application of remote sensing in support of regional disaster risk modeling", *Nat. Hazards*, **68**(1), 223-224.

DeBusk, W.M. (2010), "Unmanned aerial vehicle systems for disaster relief: Tornado Alley", *Proceedings of the AIAA Infotech@ Aerospace Conference*. Atlanta, GA, USA, April.

Dong, L. and Shan, J. (2013), "A comprehensive review of earthquake-induced building damage detection with remote sensing techniques", *ISPRS J. Photogramm*., **84**, 85-99.

Edwards, R., LaDue, J.G., Ferree, J.T., Scharfenberg, K., Maier, C. and Coulbourne, W.L. (2013), "Tornado intensity estimation: past, present, and future", *B. Am. Meteorol. Soc*., **94**(5), 641-653.

Eguchi, R.T., Huyck, C., Adams, B.J., Mansouri, B., Houshmand, B. and Shinozuka, M. (2001), *Resilient disaster response: using remote sensing technologies for post-earthquake damage detection*, Earthquake Engineering to Extreme Events (MCEER), Research Progress and Accomplishments, University of Buffalo, Buffalo, NY, USA.

FEMA.(2013), *HAZUS® -MH MR5, Multi-Hazard Loss Estimation Methodology, Hurricane Model, Technical Manual*, Federal Emergency Management Agency, Washington, D.C, USA.

Gall, M., Borden, K.A. and Cutter, S.L. (2009), "When do losses count?", *B. Am. Meteorol. Soc*., **90**(6), 799-809.

Geiß, C. and Taubenböck, H. (2013), "Remote sensing contributing to assess earthquake risk: from a literature review towards a roadmap", *Nat. Hazards*, **68**(1), 7-48.

Haan, F.L., Jr., Balaramudu, V.K. and Sarkar, P.P. (2010), "Tornado-induced wind loads on a low-rise building", *J. Struct. Eng. - ASCE*, **136**(1), 106-116.

Hamid, S. (2007), *Actuarial model for estimating insured hurricane losses*, International Hurricane Research Center, Florida International University, Miami, Florida, USA.

Harrell, F.E. (2001), *Regression Modeling Strategies: With Applications to Linear Models, Logistic Regression, and Survival Analysis*, Springer, New York, USA.

Hasegawa, H., Aoki, H., Yamazaki, F., Matsuoka, M. and Sekimoto, I. (2000), "Automated detection of damaged buildings using aerial HDTV images", *Proceedings of the IGARSS 2000. IEEE 2000 International*, Honolulu, HI, USA, July.

Hodgson, M.E., Davis, B.A. and Kotelenska, J. (2010), *Remote sensing and GIS data/information in the emergency response/recovery phase*, In *Geospatial Techniques in Urban Hazard and Disaster Analysis*, Springer, New York, USA.

Jensen, J. and Cowen, D. (1999), "Remote sensing of urban suburban infrastructure and socio-economic attributes", *Photogramm. Eng. Rem. S*., **65**(5), 611-622.

Joyce, K.E., Belliss, S.E., Samsonov, S.V., McNeill, S.J. and Glassey, P.J. (2009), "A review of the status of satellite remote sensing and image processing techniques for mapping natural hazards and disasters", *Prog. Phys. Geog*., **33**(2), 183-207.

Khorram, S., Koch, F.H., Wiele, C.F. van der and Nelson, S.A.C. (2012), *Remote sensing*, Springer Briefs in Space Development, Springer, New York, USA.

Liang, D., Cong, L., Brown, T. and Song, L. (2012), "Comparison of sampling methods for post-hurricane damage survey", *J. Homel. Secur. Emerg. Manag*., **9**(2), 11.

Marshall, T.P. (2008), "Wind speed-damage correlation in Hurricane Katrina", *Proceedings of the 88th Annual Meeting of the American Meteorological Society*, New Orleans, LA., USA.

Minor, J.E. (2005), "Lessons learned from failures of the building envelope in windstorms", *J. Archit. Eng.*, **11**(1), 10-13.

Molthan, A., Jedlovec, G. and Carcione, B. (2011), "NASA satellite data assist in tornado damage assessments", *Eos Trans. Am. Geophys. Union*, **92**(40), 337-39.

NIST. (2013), *Technical investigation of the May 22, 2011, Tornado in Joplin, Missouri*, National Institute of Standards and Technology, Gaithersburg, MD, USA.

NWS. (2011), "Joplin Tornado Event Summary - May 22, 2011", <http://www.crh.noaa.gov/sgf/? n=event_2011may22_summary>, (accessed September 21, 2013).

Pinelli, J.P., Simiu, E., Gurley, K., Subramanian, C., Zhang, L., Cope, A., Filliben, J.J. and Hamid, S. (2004), "Hurricane damage prediction model for residential structures", *J. Struct. Eng. - ASCE*, **130**(11), 1685-1691.

Radhika, S., Tamura, Y. and Matsui, M. (2012), "Use of post-storm images for automated tornado-borne debris path identification using texture-wavelet analysis", *J. Wind Eng. Ind. Aerod*., **107**, 202-213.

Simiu, E. and Scanlan, R.H. (1996), *Wind effects on structures: fundamentals and applications to design*,

(3rd Ed.), John Wiley, New York, USA.
Simmons, K.M. and Sutter, D. (2011), *Economic and societal impacts of tornadoes*, the American Meteorological Society, Boston, Massachusetts, USA.
Speheger, D.A., Doswell III, C.A. and Stumpf, G.J. (2002), "The Tornadoes of 3 May 1999: event verification in central oklahoma and related issues", *Weather Forecast*., **17**(3), 362-381.
Vickery, P.J., Skerlj, P.F., Lin, J., Twisdale Jr, L.A., Young, M.A. and Lavelle, F.M. (2006), "HAZUS-MH hurricane model methodology. II: damage and loss estimation", *Nat. Hazards*., **7**(2), 94-103.
Voigt, S., Kemper, T., Riedlinger, T., Kiefl, R., Scholte, K. and Mehl, H. (2007), "Satellite image analysis for disaster and crisis-management support", *IEEE T. Geosci. Remote*., **45**(6), 1520-1528.
WISE. (2006), *A recommendation for an enhanced fujita scale (EF-Scale)*, Wind Science and Engineering Research Center, Texas Tech University, Lubbock, Texas, USA.
Womble, J.A. (2005), *Remote-sensing applications to windstorm damage assessment*, PhD Dissertation, Texas Tech University, Lubbock, Texas, USA.
Womble, J.A., Ghosh, S., Adams, B.J. and Friedland, C.J. (2006), *Advanced damage detection for Hurricane Katrina: integrated remote sensing & VIEWS TM field reconnaissance*, MCEER Report, University of Buffalo, Buffalo, NY, USA.

JH